Strong-Motion, Site-Effects and Hazard Issues in Rebuilding Turkey: in Light of the 17 August, 1999 Earthquake and its Aftershocks

By

Mehmet Çelebi, Selçuk Toprak and Thomas Holzer
USGS (MS977)
345 Middlefield Road
Menlo Park, CA 94025
[Tel: 650-329-5623, Fax: 650-329-5163, e-mail: celebi@usgs.gov]

ABSTRACT

The August 17, 1999 Izmit (Turkey) earthquake (M_w=7.4) will be remembered as one of the largest earthquakes of recent times that affected a large urban environment (U.S. Geological Survey, 1999). The shaking that caused the widespread damage and destruction was recorded only by a handful of accelerographs in the earthquake area operated by different networks. The characteristics of these records show that the recorded peak accelerations, even those from near field stations, are smaller than expected. On the other hand, smaller magnitude aftershocks yielded larger peak accelerations. This is attributed to the sparse networks which possibly missed recording of larger motions during the main shock.

As rebuilding of Turkey starts, strong-motion networks that yield essential data must be enlarged. In addition, attention must be paid to new developments elsewhere, such as earthquake zoning maps, earthquake hazard maps, liquefaction potentials and susceptibility. This paper aims to discuss these issues.

INTRODUCTION

It is now well known that improper design and construction practices played a big role in detrimental performance of more than 20,000 structures during the August 17, 1999 (M_w=7.4) Izmit earthquake. This being a given, the main goal must be to improve design and construction practices. During this process, it is important to assess the recorded ground motions, site effects and other earthquake related hazard issues which need to be considered during rebuilding efforts.

On scale recordings of ground shaking during earthquakes are important for understanding causes of earthquake damage and the physics of fault rupture, and for advancing design codes. Approximately 38 strong motion ground records were made of the August 17, 1999 Izmit earthquake by four of the five institutions in Turkey that operate either strong motion networks or small arrays, arranged below in order of the size of their networks:

(a) The National Strong Motion Network (NSMN), operated by the Earthquake Research Department, Directorate for Disaster Affairs of the Ministry of Public Works and Settlement (ERD) [http://angora.deprem.gov.tr/],
(b) Kandilli Observatory and Earthquake Research Institute (KOERI) [http://193.140.203.8/earthqk/earthqk.html],
(c) Istanbul Technical University (ITÜ) [http://www.itu.edu.tr/].
(d) Public Water Works (DSI) – instruments dams.

[http://www.dsi.gov.tr/].

(e) Middle East Technical University (METU)
[http://www.metu.edu.tr/home/wwweerc/ and http://www.metu.edu.tr/wwwdmc/].

Of the available strong-motion ground records, 24 are from ERD, 10 are from KOERI, and 4 are from ITU. In addition, three sets of structural response records (2 from KOERI, 1 from METU) were also obtained. DSI did not retrieve any records from its dams within the earthquake region (D. Altinbilek, pers. comm., 1999). KOERI has retrieved records from the structural response arrays at Süleymaniye Mosque and Aya Sofya (Hagia Sophia) Museum [http://193.140.203.8/earthqk/earthqk.html]. METU obtained partial records from an instrumented six-story building in Gerede (P. Gülkan, *personal communication*, 1999). The largest peak acceleration at the basement of the building is 0.035 g.

The purposes of this paper are to (a) discuss essential issues related to strong-motion records of the Izmit, Turkey earthquake, (b) relate them to experiences elsewhere, and (c) deliberate on pragmatic applications in Turkey for assisting in rebuilding and (d) identify issues that must be dealt with before the next earthquake strikes the area.

STRONG-MOTION RECORDS

The Networks

The NSMN-ERD, the largest network operator in Turkey has aimed to deploy one strong-motion instrument in every major town within the earthquake zones of Turkey. This systematic effort on part of NSMN-ERD, supplemented by strong motion stations deployed by KOERI and ITU in Istanbul and Marmara Region produced very significant and important records that will be useful for studying the earthquake and rebuilding efforts. The coordinates of 19 significant stations that recorded the main-shock and the peak accelerations at these stations are summarized in Table 1. Peak accelerations of these stations are plotted into the map in Figure 1. To date, detailed site characterizations of these stations have not been documented.

Acceleration Time-Histories

Acceleration time-histories, one from each of the three networks that recorded ground motions are presented below.

In Figure 2a, the acceleration time-history of SKR (Adapazari in Sakarya Province) is shown. The station is on stiff soil. The figure exhibits more than three different shocks. Figure 2b and c shows only 40 seconds of the record re-plotted along with corresponding relative cumulative significant shaking (representative of energy) calculated by summing the square of the acceleration over time. A treatment of duration of strong shaking, following the method of Novikava and Trifunac (1994) is illustrated in Figure 2d. It is seen in these figures that the strong shaking lasts approximately 5 seconds. The main shock contributes to approximately 70% of the total significant shaking of the two shocks within the 40 seconds of the record.

In Figure 3a, the acceleration time-history of YPT (Petro-Chemical Plant in Körfez) is shown. The site is alluvial. The figure exhibits two distinctive earthquakes. Figure 3b shows the relative

cumulative significant shaking as calculated by summing the square of the acceleration over time. This figure exhibits that the strong shaking of the earthquake lasted approximately 5-6 seconds. Figure 3c shows the building that houses the strong-motion accelerograph.

A similar trend is observed in Figures 4a and b, which show the acceleration time-history and relative cumulative strong shaking of the Mecidiyeköy (MCK, within Istanbul) record. This station is on rock.

Response Spectra

Figures 5a,b and c show the response spectra and the normalized response spectra (all calculated for 5 % damping), for north-south and east-west directions, respectively, for 5 stations, including the three for which the time-history plots have been presented (Figures 2-4). These stations cover the epicentral area (stations IZT and YPT) and locations that are heavily damaged east of the epicentral area (SKR and DZC) and a location in Istanbul (MCK). IZT, YPT and DZC are on alluvial sites whereas SKR and MCK are on stiff soil and rock, respectively. The response spectra show that at different stations, the resonant periods (frequencies) change drastically. Furthermore, the normalized response spectra indicate that both YPT and DZC have long periods (low frequencies). For comparison of response spectra shapes, Figure 5c also shows the current Turkish Code response spectra for stiff soil and alluvial site conditions (Specifications for structures to be built in disaster areas, English translation by Aydinoglu, 1998). The figure indicates that for periods between 0.1-1, the design response spectra, similar to those used in the United States are challenged for this earthquake. Considering that significant majority of the structures in the epicentral area were built before this code, it becomes clear that the structures were deficiently designed in strength to resist the forces generated by the earthquake.

Taller buildings on rocky hills of Izmit and Istanbul, and the two suspension bridges in Istanbul were not affected by the long-period motions of this earthquake.

Sparcity of Strong-Motion Stations

It is our contention that the current strong-motion network in the epicentral area (and in other segments of the North Anatolian Fault and elsewhere in Turkey, for that matter) is quite sparse. Consequently, while considering shaking levels in different locations during rebuilding efforts, it is important to consider that recording of larger peak accelerations with very unique characteristics were possibly missed. This is exemplified by the following points:

1) No record of the main-shock was obtained in Gölcük and vicinity (in the immediate epicentral area). Near-fault records with large peak accelerations and long-duration pulses result in large displacements detrimental to the performance of long-period structures.
2) Only one record was retrieved from Adapazari (station SKR), which was on stiff soil in the undamaged part of Adapazari. There were no stations in the fast-growing urban/industrial areas of the Adapazari basin. The peak accelerations in the basin, almost certainly were amplified compared to that recorded at the stiff soil site. The shaking in the basin would have revealed different characteristics such as amplification due to softer layered media, basin effects and in certain areas, the effect of liquefaction that occurred.

Table 1. Coordinates and peak accelerations of stations that exhibited significant shaking.

STATION	L [g] %	T [g] %	L (+)	T (+)	V [g] %	Latitude	Longitude	Operated by
IZT	.171	.225	S	E	.146	40.790 N	29.960 E	ERD
SKR	*	.407	S	E	.259	40.737 N	30.384 E	ERD
DZC	.374	.315	W	S	.480**	40.850 N	31.170 E	ERD
IST	.061	.043	S	E	.036	41.080 N	29.090 E	ERD
GBZ	.264	.142	N	W	.199	40.820 N	29.440 E	ERD
CEK	.118	.190	N	W	.050	40.970 N	28.700 E	ERD
IZN	.092	.123	S	E	.082	40.440 N	29.750 E	ERD
BRS	.054	.046	S	E	.025	40.183 N	29.131 E	ERD
YPT	.230	.322	W	N	.241	40.763 N	29.761 E	KOERI
ATS	.252	.180	N	W	.081	40.980 N	28.692 E	KOERI
DHM	.090	.084	S	W	.055	40.982 N	28.820 E	KOERI
YKP	.041	.036	S	W	.027	41.081 N	29.007 E	KOERI
FAT	.189	.162	S	E	.131	41.054 N	28.950 E	KOERI
ARC	.211	.134	N	W	.083	N/A ***	N/A ***	KOERI
HAS	.056	.110	S	E	.048	40.869 N	29.090 E	KOERI
MCK	.054	.070	N	W	.038	41.065 N	28.990 E	ITÜ
ZYT	.120	.109	N	W	.051	40.986 N	28.908 E	ITÜ
MSK	.054	.038	N	W	.031	41.104 N	29.010 E	ITÜ
ATK	.103	.168	N	W	.068	40.989 N	28.849 E	ITÜ

L-Longitudinal, T-Transverse, V-Vertical [Note: The components L and T are the instrument components. They do not correspond to North-South and East-West automatically. The reader is referred to the information in this table and from each network to obtain the correct orientation of each horizontal component of the record of interest]. * L component did not function, ** based on a single spike (actual value may be smaller), *** coordinates not provided

3) During the main shock of the August 17, 1999 earthquake, the largest recorded peak accelerations (SKR, 0.41 g horizontal and Düzce, 0.48 g vertical) were most likely not the largest that actually occurred. Figure 6 shows time-history plots recorded during the M_s=5.7 aftershock of 13 September 1999 at a temporary station, Tepetarla (near Izmit) with large peak accelerations. In particular, the record from Tepetarla shows peak acceleration of ~ 0.6 g, larger than any peak recorded during the main shock. Furthermore, during the November 12, 1999 (Ms=7.2) Duzce event, one of the stations (Bolu) recorded 0.8 g (EW).
4) Furthermore, Figure 7 shows that in California, the recording of larger shaking (in terms of peak acceleration) increased as the number of accelerographs deployed by the State of California and USGS increased. The trend that larger number of deployments increase the ability to capture larger peak accelerations is very clear. In this figure, records with large peak accelerations obtained in Canada (1985 Nahanni) and Japan (1995 Kobe) earthquakes are included for comparison.

Attenuation

In general, the recorded peak accelerations fared well with peak accelerations estimated from attenuation curves calculated for a M=7.4 earthquake. For illustration only, the peak values from the 19 stations in Table 1 are superimposed on the attenuation curves in Figures 8a and b plotted for two types of soils (shear wave velocity, V_s =760m/s and V_s=360m/s). However, this should be interpreted in light of the sparse deployment discussed above (that may have resulted in missing motions with larger peak accelerations) and also the fact that considerable number of the stations listed in the table are recorded in buildings that are more than two stories and should not be in the comparative curves. The cutoff number of stories used in the data base for the regression analyses in deriving the attenuation curves is two (Boore, Joyner and Fumal, 1997). For example, Figure 3d shows the three story building that housed the YPT station.

AFTERSHOCK DEPLOYMENTS

While the strong-motion network was not dense enough to reveal the effect of ground shaking on the structures, deployment of limited number of temporary arrays have produced valuable information on explaining site effects at various locations. USGS deployed a number of accelerometers and velocity transducers at the South side of Izmit Bay including Golcuk, Ford Plant and Yalova. Figure 9 is a sample seismogram of an aftershock obtained from the Golcuk area including the Ford Plant depicting the variability of ground motion at short distances (<1 km) (Çelebi, Dietel and Glassmoyer, 1999). Another deployment result showing site effects is summarized by Cranswick and others (1999).

OTHER ISSUES

Soil-Structure Interaction

The majority of the building inventory on alluvium media were most likely subjected to soil-structure interaction effects (SSI). The buildings with 1-8 stories had very small or no embedment. Most were constructed on continuous beam foundations. This is particularly important for those structures that had little or no embedment (D) as compared to the height (H) or width (L) of a building ($0< D/H<0.5$). Aviles and Perez-Rocha (1998) recently showed (Figure 10) that the effective period of structures can increase by a factor of 2 for H/L~3. In this figure, accepting $T_h=H/(V_sT)$ as relative measure of relative stiffness of the structure to that of the soil. T_h can be approximated as T_h~$30/V_s$ (for average 3 m height per story and T~0.1 N, (N number of stories) for most structures. For V_s =300, T_h~0.1 and for softer soils with V_s =60 m/s, T_h~0.5. The figure also shows that effective damping reduces considerably. These affect adversely the performance of structures. In rebuilding, embedment and foundation issues must be addressed.

Near-Fault Issues and pulses

In recent years, particularly during the 1994 Northridge and 1995 Kobe earthquakes, significant number of records with large peak accelerations (*e.g.* ~1 g) and with long-duration pulses have been acquired in the near field (<10 km) from the fault. Consequently, to compensate for the additional demand in design strength caused by such motions, recent codes in the United States

adopted the Near Fault Factors (UBC, 1997). Thus, the seismic zoning factors are effectively increased by a factor, $1<N<2$ for seismic zone 4 (the highest seismic risk zones in the United States) within 10 km of those fault zones that are capable of generating (a) $M \geq 7$ earthquakes with slip rates exceeding 5 mm/year or (b) earthquakes $M \geq 6.5$ with slip rates smaller than 5 mm/year[1]. The North Anatolian Fault (NAF) is tectonically similar to the San Andreas Fault in California; therefore, such factors should also be considered in selective zones along the NAF. The recorded responses clearly show long period pulses (~5 sec in case of YPT record) (see spectra).

Liquefaction

Liquefaction-induced ground failures caused sinking and settlement of buildings in several localities, including Adapazari, Gölcük, and Sapanca, during the August 17, 1999 earthquake. The combination of the seismic, geologic and geotechnical conditions of these localities controls the occurrence of liquefaction.

Liquefaction can occur at significant distances from an earthquake source. Ambraseys (1988) compiled worldwide data from shallow earthquakes to estimate a limiting distance to seismic source beyond which liquefaction has not been observed. Figure 11a shows Ambraseys' data and the curve that bounds the data. The figure shows that liquefaction can be expected at greater distances with increasing earthquake magnitude. Ambraseys' bound can be considered only as a first approximation for regional liquefaction hazard predictions.

Experience from past earthquakes shows that certain geologic settings are more prone to liquefaction than others. Shallow, saturated Holocene fluvial, deltaic and aolian deposits and poorly compacted artificial sand fills have highest susceptibilities to liquefaction (Youd and Hoose, 1977). Geologic setting maps are useful for regional liquefaction susceptibility studies. But they are not substitutes for site-specific evaluations of liquefaction hazard.

The "simplified procedure" introduced by Seed and Idriss (1971) is used commonly to assess the liquefaction potential of cohesionless soils. This procedure has been revised and augmented over

[1] In the Uniform Building Code, the total design base shear in a given direction is determined from the following formula: $V = [C_v I / R T] W$, where C_v is is the seismic coefficient (for zone 4, is given by $0.32N_v$, $0.40N_v$, $0.56N_v$, $0.64N_v$, $0.96N_v$ for soil profile types S_A [shear wave velocity, $V_s>1500$ m/s] , S_B [$760< V_s <1500$ m/s], S_C [$360< V_s <1500$ m/s], S_D[$180< V_s <360$ m/s] and S_E [$V_s <180$ m/s] respectively), I is the importance factor, R is the ductility factor, T is the fundamental period of the design structure and W is the weight of the structure. The total design base shear is not to exceed $V=[2.5C_a I/ R]W$ but is not to be less than $V=[0.11C_a I W]$ where C_a is the seismic coefficient and similarly ranges as $0.32 N_a$, $0.40N_a$,$0.40N_a$, $0.44N_a$ and $0.36N_a$ for the soil profiles S_A, S_B,S_C, S_D and S_E respectively. Furthermore, for Seismic Zone 4, the total base shear shall also not be less than the following: $V=[0.8ZN_vI/R]W$. Z is the seismic zone factor and is 0.4 for zone 4. In the above, $1<N_v <2$ and $1<N_a<1.5$] and are interpolated from tables according to different type of soil profiles and distance from fault. The highest factors are for sites less than 2 km from the faults. (Uniform Building Code, 1997).

the past years (e.g. Seed and others, 1983; Youd and Idriss, 1997). The simplified procedure requires calculation or estimation of two variables, namely cyclic stress ratio (CSR) and cyclic resistance ratio (CRR). CSR corresponds to the seismic demand placed on a soil layer whereas CRR corresponds to the capacity of the soil to resist liquefaction. CSR can be calculated by using the following equation (Seed and Idriss, 1971):

$$CSR = (\tau_{av}/\sigma'_{vo}) = 0.65\,(a_{max}/g)(\sigma_{vo}/\sigma'_{vo})r_d \qquad (1)$$

where a_{max} is the peak horizontal acceleration at ground surface generated by the earthquake, g is the acceleration of gravity, σ_{vo} and σ'_{vo} are total and effective vertical overburden stresses, respectively, and r_d is a stress reduction coefficient. The latter coefficient provides an approximated correction for flexibility of the soil profile. The average value for r_d typically varies between 1.0 at the surface to 0.9 at 10 m depth.

CRR is determined by using empirical relationships developed from past earthquake data (e.g. Seed and others, 1983; Youd and Idriss, 1997). The empirical relationships, which were originally based on SPT, have been extended to include CPT (e.g. Robertson and Campanella, 1985; Seed and DeAlba, 1986; Robertson and Wride, 1997). A recent summary and update of the simplified procedure are described in Youd and Idriss (1997).

As an example, Figure 11b shows the worldwide CSR data with respect to clean sand equivalent SPT blow count, $(N_1)_{60cs}$ (Toprak, et al., 1999). All CSR's were adjusted to M_w7.5 with the earthquake magnitude scaling factors (MSF) developed by I. M. Idriss (Youd and Idriss, 1997). The fines content correction of SPT blow counts to clean sand equivalent blow counts were made according to Youd and Idriss (1997). Also shown in the figure is the clean sand liquefaction boundary curve for M_w7.5. The boundary curve distinguishes reasonably well between liquefaction and nonliquefaction sites. Similar curves based on CPT can also be used to evaluate liquefaction resistance.

These methods (and others) can be used to assess the liquefaction potential in areas such as Adapazari and elsewhere for land use planning or to take appropriate design precautions.

Fault Rupture Zoning and Implications for Turkey

The experiences in California related to fault rupture zones is particularly appropriate to be considered for Turkey also. The NAF and San Andreas Faults are similar and have and will produce significant earthquakes. Figure 12 illustrates the similarities both in length of the faults and the strike-slip mechanism.

In 1972, following the 1971 San Fernando earthquake in California, the California State Assembly passed the Alquist-Priola Earthquake Fault Zoning Act. The purpose of the law was to prevent construction on or near the surface fault rupture zones. It led to establishment of offset distances from the surface fault rupture zones. During the 17 August 1999 earthquake, numerous buildings and industrial plants were adversely affected because they were on or near the fault

surface rupture zones. Turkey must establish such zones to be used by municipalities and provinces to prevent construction within the fault zones. A sample fault zone map is shown in Figure 13. The Alquist Priola Act is provided in Appendix A.

In 1990, in California, another significant act, Seismic Hazards Mapping Act was adopted. The important aspect of this act is summarized in this quotation: " The Legislature finds and declares all of the following: (a) The effects of strong ground shaking, liquefaction, landslides, or other ground failure account for approximately 95 percent of economic losses caused by an earthquake, (b) Areas subject to these processes during an earthquake have not been identified or mapped statewide, despite the fact that scientific techniques are available to do so, (c) It is necessary to identify and map seismic hazard zones in order for cities and counties to adequately prepare the safety element of their general plans and to encourage land use management policies and regulations to reduce and mitigate those hazards to protect public health and safety."

Figure 14 shows a sample seismic hazard map.

CONCLUSIONS

1. The strong-motion network on the North Anatolian Fault is very sparse. Denser arrays are necessary in urban areas. The arrays should be supplemented with downhole accelerographs and piezometer arrays in liquefaction susceptible areas. For example, in Adapazari, only one triaxial accelerograph was in operation. It was located at a stiff soil site – older part of that town. A single record was obtained from this station (minus a component due to malfunction). On the other hand, the majority of the settlement in the town had grown in the last three decades into the alluvial basin. The absence of records from the basin makes it difficult to correlate the extensive damage and liquefaction with the strong shaking. Therefore, it is important to increase the number of accelerographs in urban environments to cover different geological settings so that the actual motions in the basins and heavily damaged areas can be recorded.
2. Detailed site-characterization of the stations are not known. A systematic effort should be embarked upon to characterize the sites.
3. The number of instrumented structures was minimal. In the future, instrumentation of typical structures in the area will reveal the progression of inelastic behavior for the structures that are typical to this area.
4. In selected zones of the NAF, near-fault factors that increase the seismic coefficients in the codes must be considered.
5. Whenever applicable (e.g. in Adapazari basin), special site-specific design response spectra should be developed.
6. Soil-structure interaction effects possibly adversely affect the performance of the 4-8 story stiff structures (typically reinforced concrete framed buildings with infill walls) in the alluvial basin in Turkey. Most of these buildings have small embedment. Foundations must be properly designed to reduce the adverse effect of such interaction.

REFERENCES

Ambraseys, N. N., 1988, Engineering seismology: Earthquake Engineering and Structural Dynamics, v. 17, no. 1, 1-105.

Aviles, J., and Perez-Rocha, L. E., 1998, Effects of foundation embedment during building-soil interaction, Int'l journal of Earthquake Eng. Struct. Dyn., 27, 1523-1540.

Boore, D. M., W. B. Joyner, and T. E. Fumal, 1997, Equations for estimating horizontal response spectra and peak acceleration from western North American earthquakes: A summary of recent work, Seismological Research Letters, v. 68, 128-153.

Çelebi, M., Dietel, C., and Glassmoyer, G., 1999, A Prelimanary report on the Aftershock Measurements following the Izmit (Turkey) earthquake of August 17, 1999 – in and near Golcuk and Ford-Otosan Plant Site, USGS Open-File report (*in preparation*)

Cranswick, E., Ozel, O., Meremonte, M., Erdik, M., Safak, E., Mueller, C., Overturf, D., and Frankel, A., 1999, Earthquake Damage, Site Response, and Building Response in Avcilar, West of Istanbul, Turkey, paper submitted to the Intern'l Conf. on the Kocaeli Earthquake: A Scientific Assessment and Recommendations for Re-Building, organized by Istanbul Technical University and International Association for housing Science (USA).

Novikava, E. I., and Trifunac, M. D., 1994, Duration of ground motion in terms of earthquake magnitude, epicentral distance, site conditions and site geometry, Journal of Earthquake Engineering and Structural Dynamics, 23, 1023-1043.

Robertson, P.K., and Campanella, R.G., 1985, Liquefaction potential of sands using the CPT: Journal of Geotechnical Engineering, v. 111, no. 3, 384-403.

Robertson, P.K., and Wride, C.E., 1997, Cyclic liquefaction and its evaluation based on the SPT and CPT, *in* Youd, T.L., and Idriss, I.M., eds., Evaluation of liquefaction resistance of soils, Salt Lake City, UT, National Center for Earthquake Engineering and Research Technical Report 97-0022, 41-87

Seed, H. B., Idriss, I. M., and Arango, I., 1983, Evaluation of liquefaction potential using field performance data: Journal of Geotechnical Engineering, v. 109, no. 3, 458-482.

Seed, H. B., and DeAlba, P., 1986, Use of SPT and CPT tests for evaluating the liquefaction resistance of sands, in Clemence, S.P., (ed.), ASCE Geotechnical Special Publication No. 6, 281-301.

Seed, H. B., and Idriss, I.M., 1971, Simplified procedure evaluating soil liquefaction potential: Journal of Soil Mechanics and Foundation Engineering, v. 97, no. 9, 1249-1273.

Specification for Structures to be Built in Disaster Areas , Ministry of Public Works and Settlement Government of Republic of Turkey, *Issued on: 2.9.1997, Official Gazette No.23098, Effective from: 1.1.1998, Amended on: 2.7.1998, Official Gazette No.23390 (English translation by N.* Aydinoglu, 1998).

Toprak, S., Holzer, T.L., Bennett, M. J., Tinsley, J. C. III, 1999, CPT- and SPT-based probabilistic assessment of liquefaction potential, Proceedings of seventh US-Japan workshop on earthquake resistant design of lifeline facilities and countermeasures against liquefaction, Seattle, August 15-17, 1999, Multidisciplinary Center for Earthquake Research (Preprint).

U. S. Geological Survey, 1999, Implications for earthquake risk reduction in the United States from the Kocaeli, Turkey, earthquake of August 17, 1999: U.S. Geological Circular 1193, *in press*.

Uniform Building Code, 1997, International Conference of Building Officials, Whittier, Ca.
Youd, T. L., and Hoose, S. N., 1977, Liquefaction susceptibility and geologic setting: Proceedings of the sixth world conference on earthquake engineering, New Delhi, India, v. 3, 2189-2194.
Youd, T. L., and Idriss, I. M. (eds.), 1997, Proceedings of the NCEER workshop on evaluation of liquefaction resistance of soils, Salt Lake City, UT, National Center for Earthquake Engineering and Research Technical Report 97-0022, 276 p.

Web Pages:

ERD: [http://angora.deprem.gov.tr/],
KOERI: [http://193.140.203.8/earthqk/earthqk.html],
ITÜ [http://www.itu.edu.tr/].
DSI : [http://www.dsi.gov.tr/)].
METU: [http://www.metu.edu.tr/home/wwweerc/`and http://www.metu.edu.tr/wwwdmc/].

APPENDIX A: SHOULD TURKEY ESTABLISH ACTS EQUIVALENT TO ALQUIST-PRIOLA ACT OF CALIFORNIA?

The following are quoted from : http://www.consrv.ca.gov/dmg/rghm/a-p/releases/mpnp.htm and http://www.consrv.ca.gov/dmg/rghm/a-p/ap-intro.htm

"The Alquist-Priolo Eartrhquake Fault Zoning Act was passed in 1972 to mitigate the hazard of surface faulting to structures for human occupancy. This state law was a direct result of the 1971 San Fernando Earthquake, which was associated with extensive surface fault ruptures that damaged numerous homes, commercial buildings, and other structures. Surface rupture is the most easily avoided seismic hazard."

"The Alquist-Priolo Earthquake Fault Zoning Act's main purpose is to prevent the construction of buildings used for human occupancy on the surface trace of active faults. The Act only addresses the hazard of surface fault rupture and is not directed toward other earthquake hazards. The Seismic Hazards Mapping Act, passed in 1990, addresses non-surface fault rupture earthquake hazards, including liquefaction and seismically induced landslides."

"The law requires the State Geologist to establish regulatory zones (known as Earthquake Fault Zones) around the surface traces of active faults and to issue appropriate maps. ["Earthquake Fault Zones" were called "Special Studies Zones" prior to January 1, 1994.] The maps are distributed to all affected cities, and state agencies for their use in planning and controlling new or renewed construction. Local agencies must regulate most development projects within the zones. Projects include all land divisions and most structures for human occupancy. Single family wood-frame and steel-frame dwellings up to two stories not part of a development of four units or more are exempt. However, local agencies can be more restrictive than state law requires Before a project can be permitted, cities and counties must require a geologic investigation to demonstrate that proposed buildings will not be constructed across active faults. An evaluation and written report of a specific site must be prepared by a licensed geologist. If an active fault is found, a structure for human occupancy cannot be placed over the trace of the fault and must be set back from the fault (generally 50 feet)."

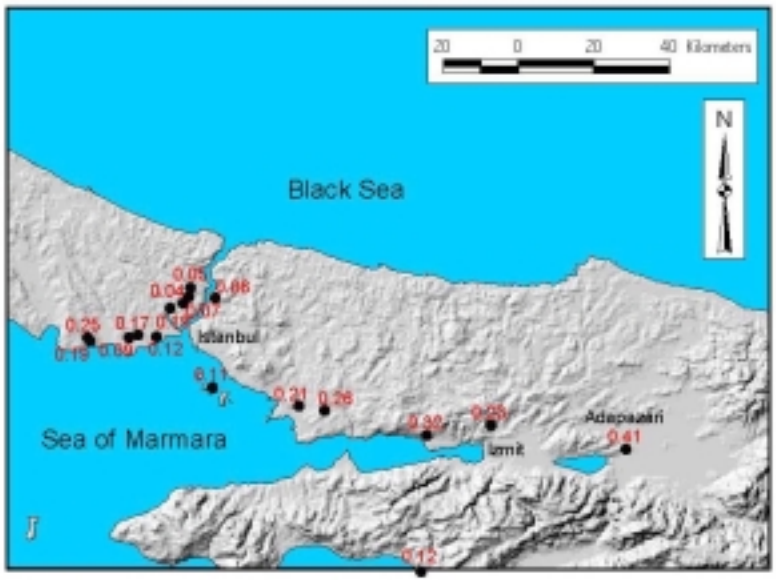

Figure 1. Map showing peak accelerations summarized in Table 1 plotted at relative locations of significant strong-motion stations within and in close proximity to the epicentral area (Base map courtesy of BKS Surveys Ltd., N. Ireland).

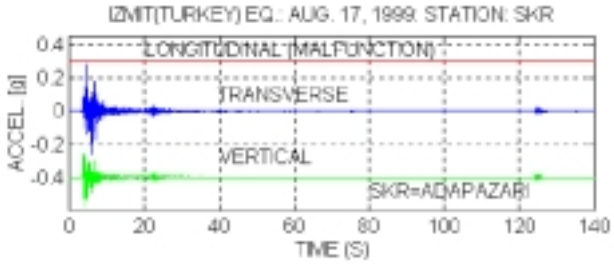

Figure 2 (a): Time-history of SKR record (Longitudinal component malfunctioned). The plot shows several events.

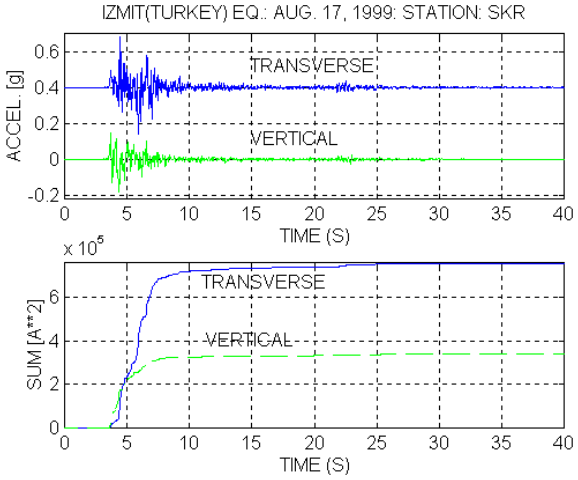

Figure 2 (b) Only 40-second window of the acceleration record re-plotted to show (c) thesignificant strong shaking, almost all by the first shock and indicating the duration of strong-shaking as 5-6 s.

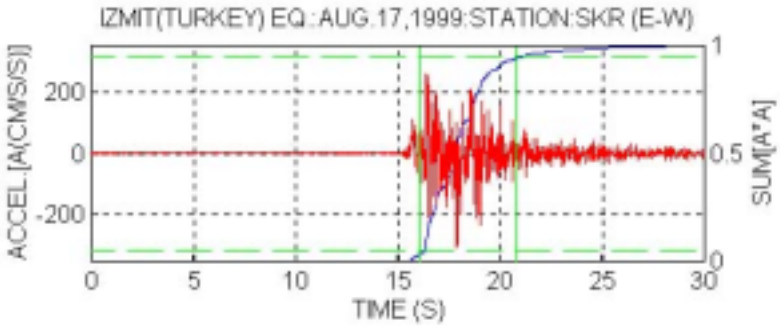

Figure 2 (d) Definition of duration of strong shaking (time between 5-95% of the relative cumulative squared acceleration) [Reference: Novikava and Trifunac, 1994].

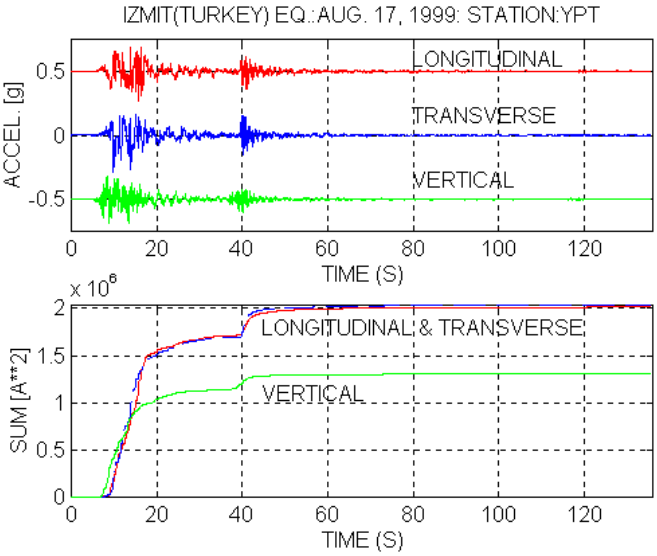

Figure 3a and b. Time-history of YPT. The plot shows the second event approximately 30-seconds after the first and (b) the significant strong shaking of the mainshock contributes approximately 70 % of the total and the strong shaking duration is 5-6 s. (c) Picture of the three-story building that housed the accelerograph of the YPT station.

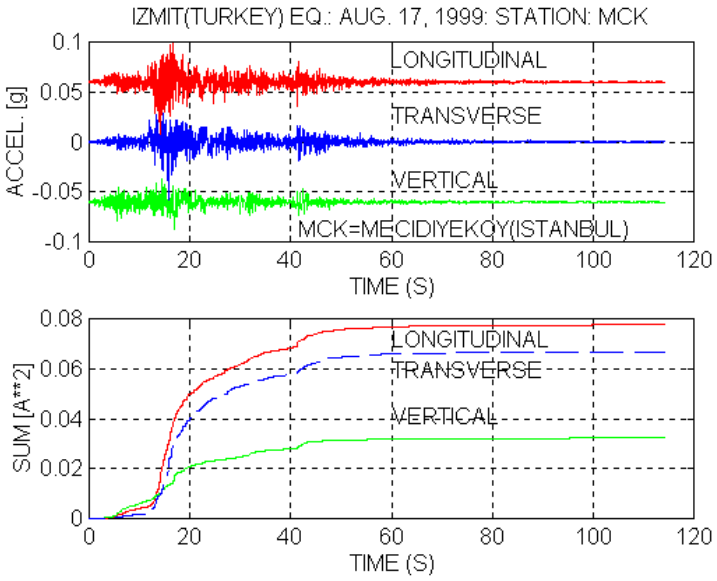

Figure 4a and b. Time-history of MCK (in Istanbul) record. (b) the significant strong shaking of the mainshock contributes approximately 70 % of the total and the strong shaking duration is again 5-6 s.

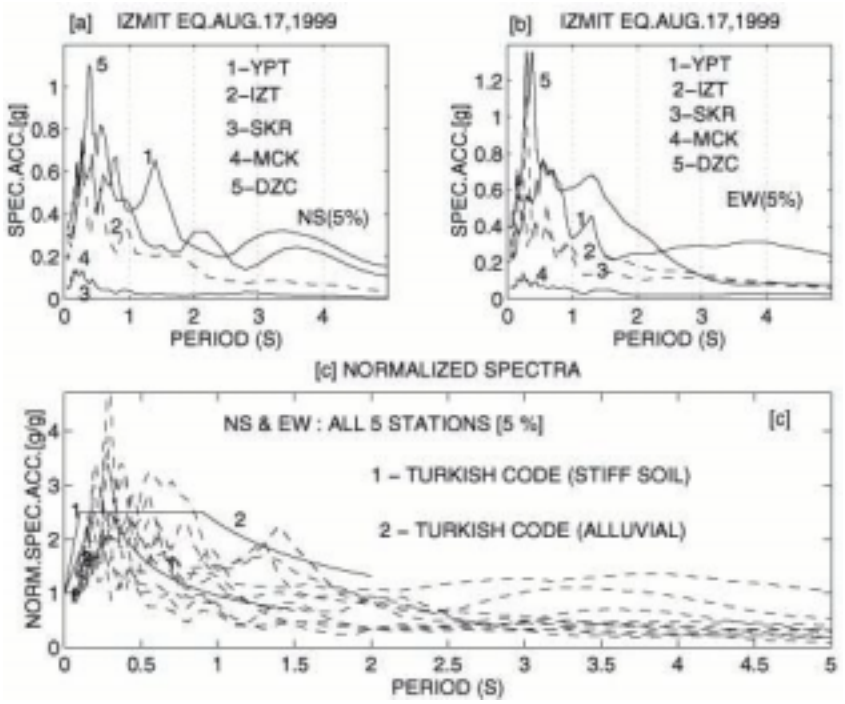

Figure 5. (a and b) Response spectra (5 % damped) for 5 stations and (c) Normalized response spectra of 5 stations compared with design response spectra of Turkish Code (1998).

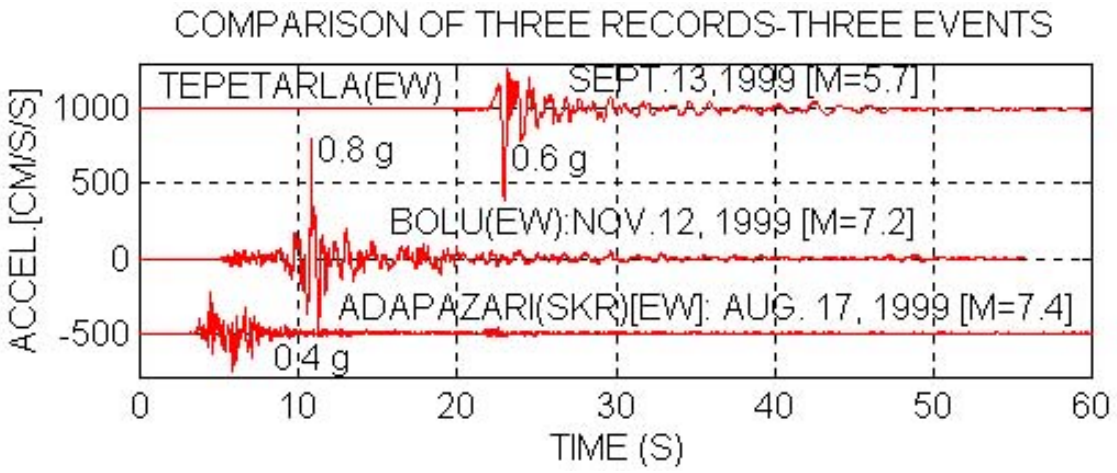

Figure 6. Peak accelerations for the August 17, 1999 main shock and two aftershocks, each recorded at a different location.

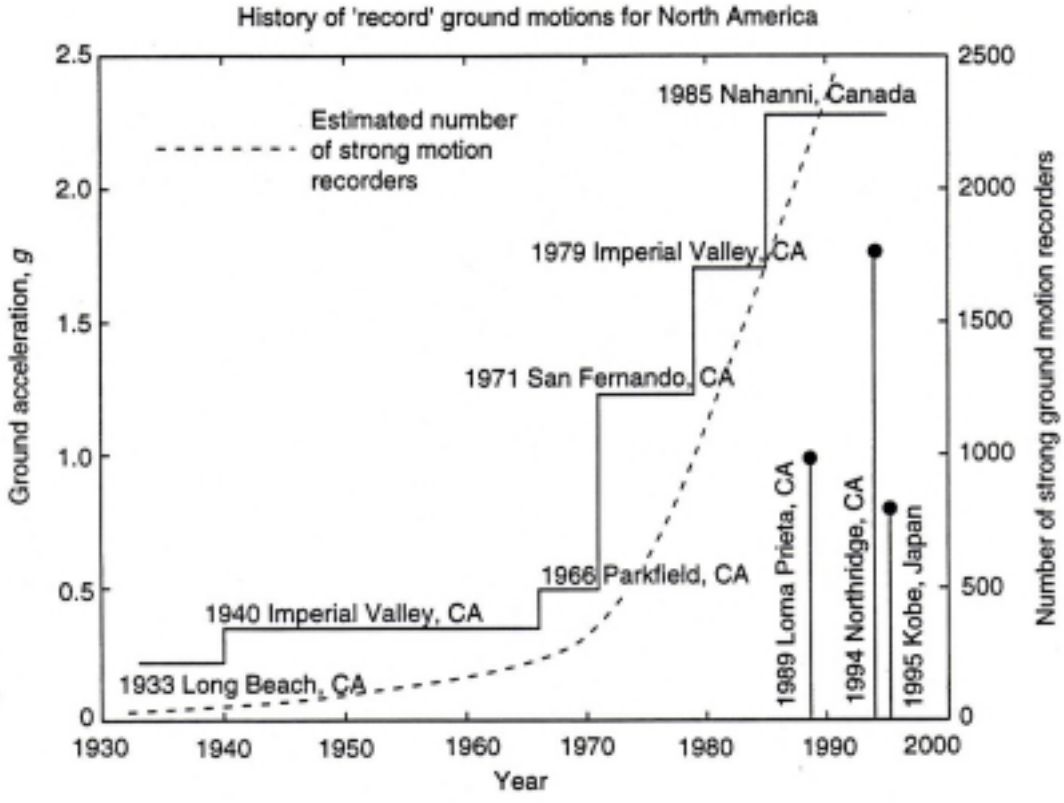

Figure 7. Schematic showing the increase in recorded peak accelerations with increase in the number of accelerographs.

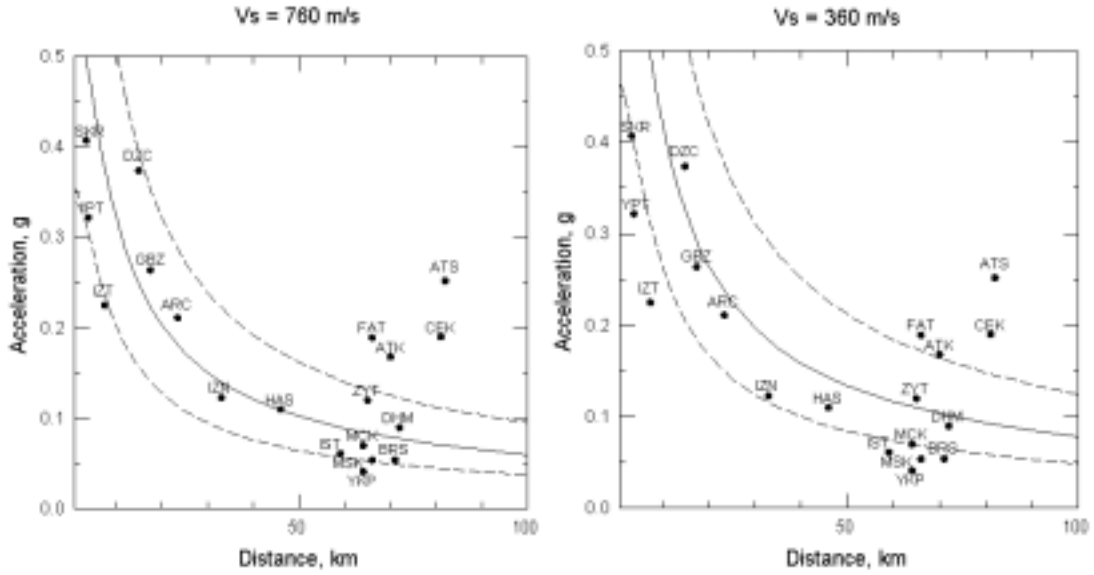

Figure 8. Attenuation curve for an M=7.4 earthquake superimposed with peak accelerations in Table 1 (plotted using method from Boore, Joyner and Fumal, 1997).

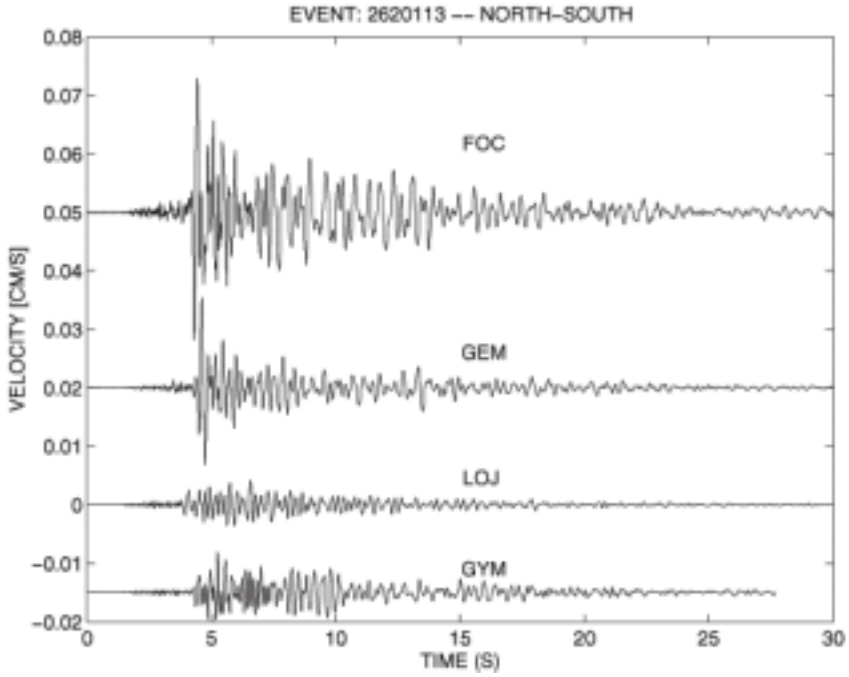

Figure 9. The seismograms shows relative amplitudes of velocity records at close distances (<1km). The stations FOC, GEM and LOJ are within the Ford Plant Grounds near Gölcük. Station GYM is within 1 km to these stations.

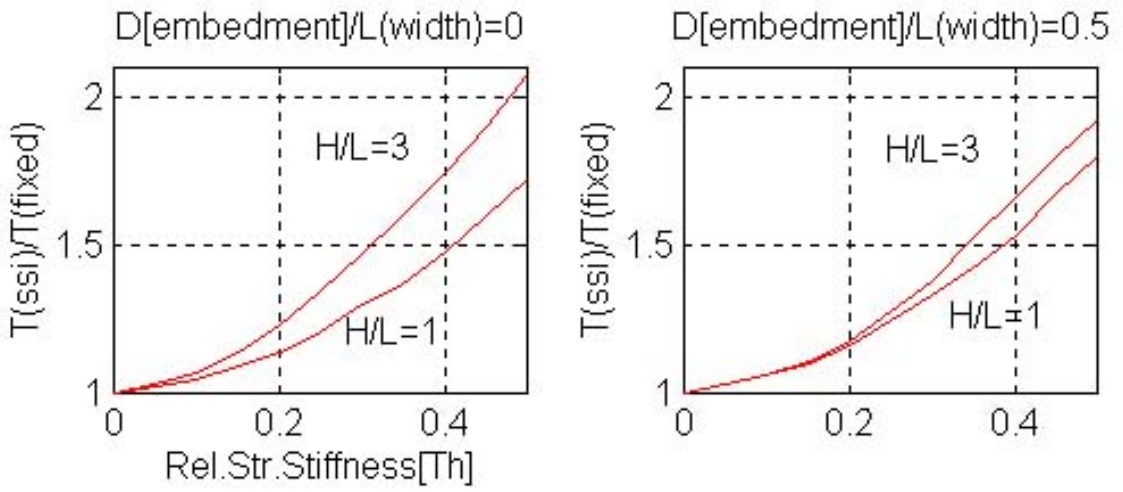

Figure 10. Effect of foundation embedment on structural period when soil-structure interaction is included (redrawn from Aviles and Perez-Rocha, 1998).

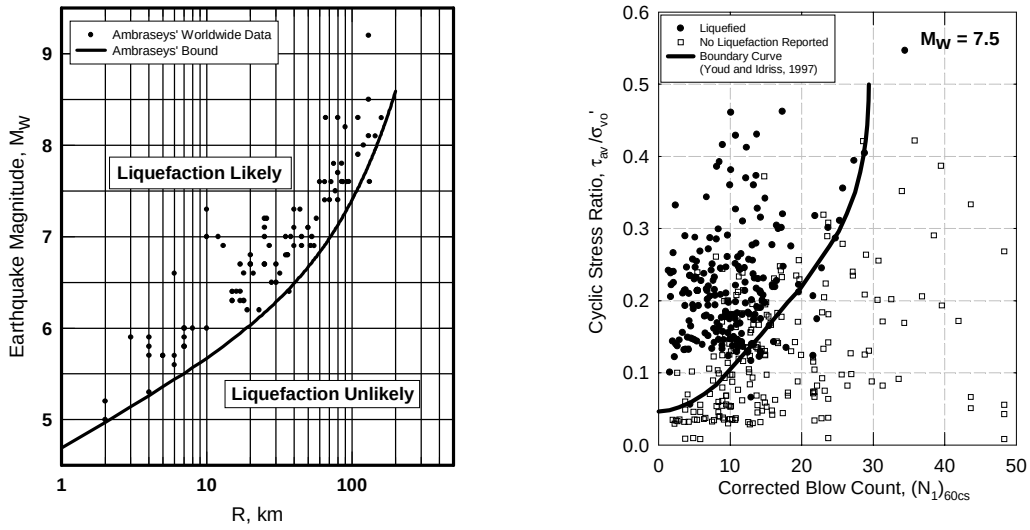

Figure 11 (a-left) Relationship between distance from the earthquake source to furthest liquefied site and moment magnitude (after Ambraseys, 1988) and (b-right) SPT-based liquefaction prediction (after Toprak, et al., 1999).

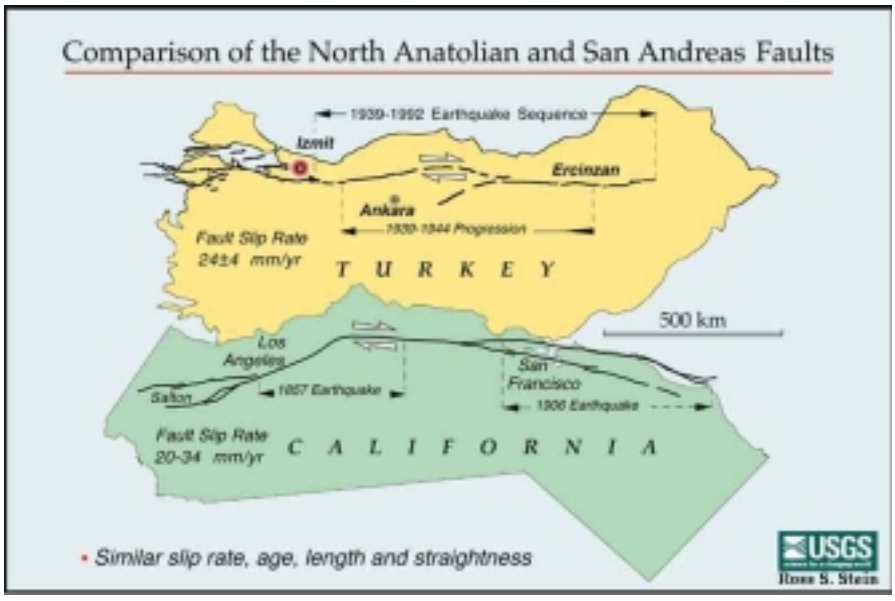

Figure 12. Comparison of North Anatolian and San Andreas Faults [from http://quake.wr.usgs.gov/study/turkey/#photos].

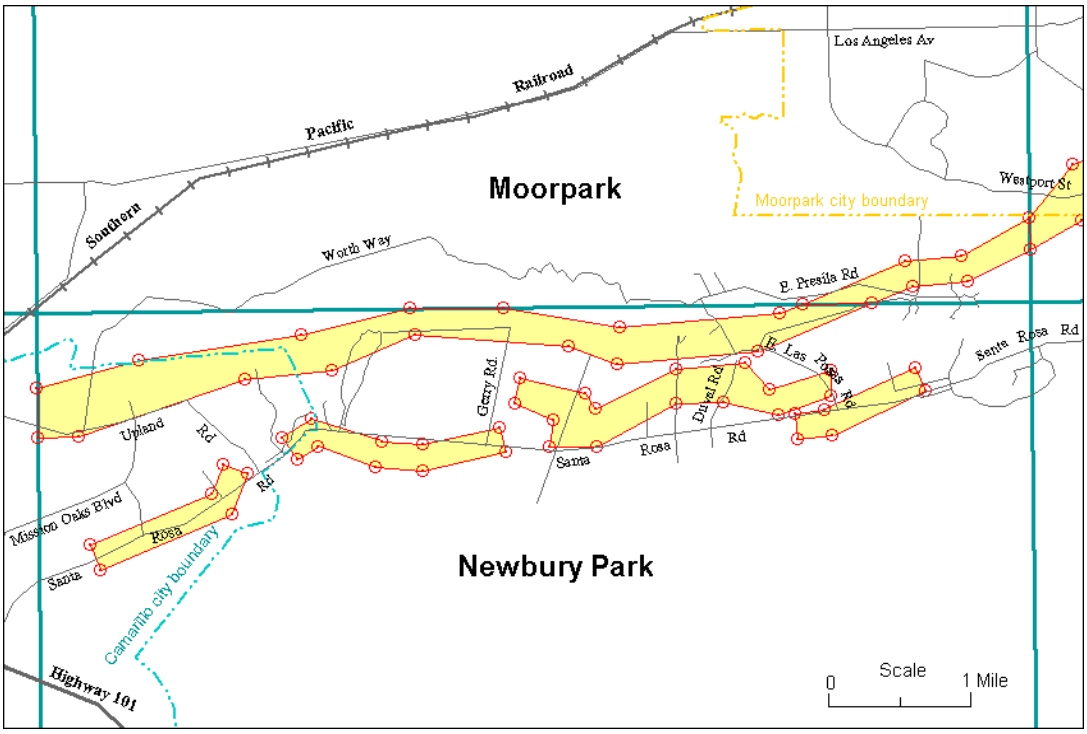

Figure 13. Sample Earthquake Fault Zone Map [from: http://www.consrv.ca.gov/dmg/rghm/a-p/releases/mpnp.htm] Official Earthquake Fault Zones (EFZ) encompass traces of the Simi-Santa Rosa fault zone (not shown here). EFZs are shown in yellow; EFZ boundaries are shown as red circles connected by straight red line segments. The city boundary of Camarillo is delineated in light blue and Moorpark is shown in yellow.

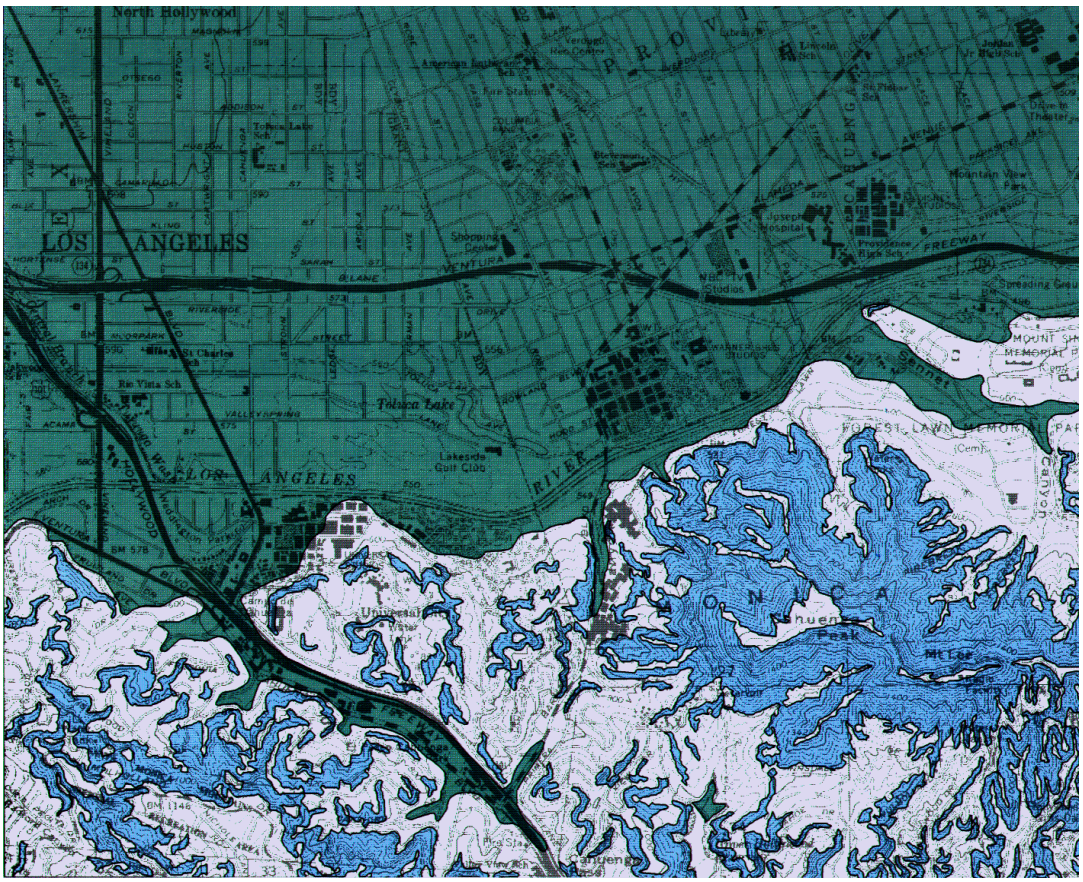

Figure 14. A sample hazard map showing liquefaction(green) and landslide (blue) susceptible areas (from http://www.consrv.ca.gov/dmg/shezp/maps/m_bur5.htm)